L-SHAPED GRAVITY WALLS. RECOMMENDED PRACTICE FOR ULS

N. Mortensen[1], **J.S. Steenfelt**[2]

KEYWORDS

Gravity walls, non-associated flow versus associated flow, water pressures.

ABSTRACT

The scope of the present paper is to identify key issues that should be considered during the design of L-shaped gravity walls. Results from the finite element method have been combined with a tailor-made software code to investigate relevant mechanisms to be included in the recommended approach. The main elements addressed are the failure mechanism along the rear side wall and added robustness in the design. The paper suggests a simple design approach that will provide safe structures without undue conservatism.

1. INTRODUCTION AND BACKGROUND

When designing L-shaped gravity walls in the ultimate limit state (ULS), cf. Figure 1, equilibrium shall be ensured considering passive earth pressures in the front of the wall, active earth pressures along the rear side of the wall, water pressures and bearing capacity of the base of the wall. The failure mode of L-shaped gravity walls may be characterized by horizontal sliding or lack of bearing capacity caused by overturning moment; examples of the latter are illustrated on Figure 1.

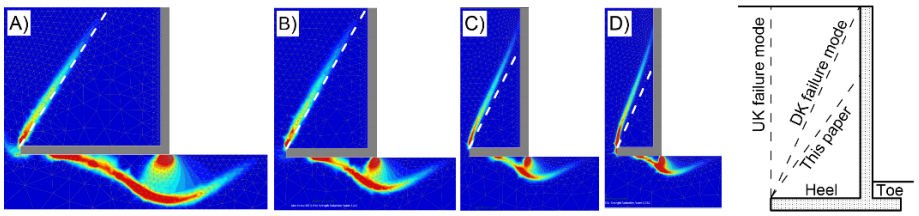

Figure 1 Contour plots of mobilised shear stress as found by the finite element method in coarse grained soils. The white dashed lines are inclined corresponding to the statically admissible angle, 45°-φ'/2 (active failure boundaries).

[1] Geotechnical Director, nmGeo
[2] Technical Director, COWI

Most countries agree on the passive pressure, but active pressures are applied differently from country to country and deviations are also observed considering the bearing capacity. Design practice from Denmark (DK) and the United Kingdom (UK) is illustrated on the right hand side of Figure 1. The DK approach is to apply a fully rough active pressure on the line between the rear side of the heel and the top of the wall, while the UK approach is to a apply a smooth active pressure on the vertical line through the rear side of the heel.

Cases included in this paper is limited to a study of coarse grained soil (zero effective cohesion) with unit weight, a possible surcharge load, horizontal soil surface and water tables being placed below the zone of influence. The principles about including water tables are, however, included.

2. METHODOLOGY

The finite element method

Two different software packages were applied in this work, Optum^{G2}, [1] and Plaxis 2D, [2] using 15-node triangular elements. The soil is modelled using a drained Mohr-Coulomb associated flow failure criterion and a secant value of the peak friction angle, φ'. A total unit weight of 20 kN/m^3 has been applied together with Young's modulus, E = 35 MPa and Poisson's ratio, ν = 0.30. Interface elements with a strength of δ = φ' are placed in the contact zone between soil and structure. A linear elastic material is used for the concrete wall applying E = 20,000 MPa, ν = 0.20 and a total unit weight of 24 kN/m^3. The thickness of concrete elements has been set to 0.30 m.

Limit equilibrium method

A limit equilibrium method has been established to solve the ULS case and the main aspects are illustrated on Figure 2.

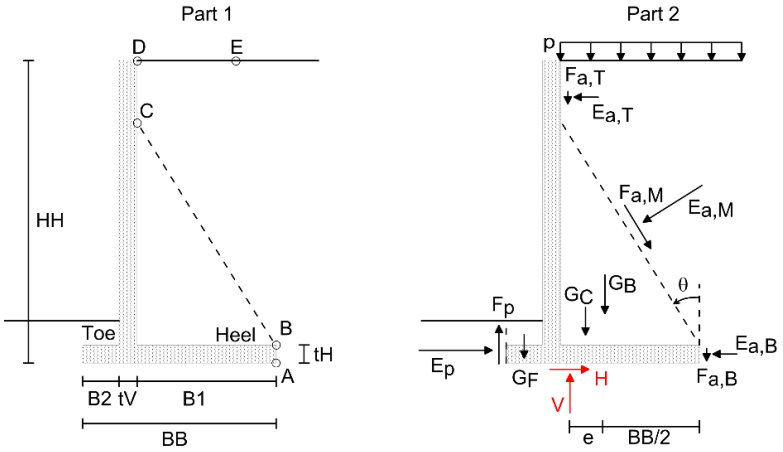

Figure 2 Part 1: Applied geometry of L-shaped gravity wall. Part 2: Actions on the wall together with the reactions H and V at the base.

A computer code is developed to conduct the calculations using a geometry as defined on Figure 2, Part 1. When the DK approach is investigated, the rear side rupture line goes along the points ABD, assuming a completely rough interface. For the UK approach, the bounding rupture line extends vertically from point A (smooth interface). A third failure mode is investigated where the rupture line runs along AB, and then along a line inclined θ with vertical so it may intersect the wall (e.g. point C) or the soil surface (e.g. point E), assuming a completely rough interface. An optimization routine is included in the third failure mode where the maximum overturning moment around point A is sought by varying θ and using this overturning moment to establish the required vertical reaction.

Figure 2, Part 2, shows the actions considered and the sum of actions shall be counteracted by reactions complying with vertical and horizontal equilibrium together with moment equilibrium in accordance with EN 1997-1 (reactions are marked in red on Figure 2). The overturning moment is evaluated with reference to point A. The symbol G_C refer to the weight of the wall, G_F is the weight of the soil on top of the toe and G_B is the weight of the soil at the rear side. The vertical surcharge load contributes with a vertical component provided that the value of θ causes the rupture line to intersect the soil surface to the right of point D. Each of these components (and the associated point of application) are estimated together with the total passive and active earth pressures (tangential components included) acting on the wall. Soil resistance relies on effective stresses while G_C, G_F and G_B should be based on total unit weights and a water pressure following Section 4 (not included in current calculations).

Projecting all actions on a horizontal plane leads to the horizontal reaction, H and similar for the vertical reaction, V. The estimated moment around point A, MoA is used to derive the eccentricity, e using $MoA = V \cdot (e + BB/2)$. The calculation procedure above may be wrapped in a zero-seeking procedure where the heel length, B1, is changed until the vertical pressure caused by V over the effective foundation width equals the computed bearing capacity or until the sliding condition ($\tan\varphi' = H / V$) is met, whichever is most critical for the structure in question. The output from the suggested approach is therefore the minimum foundation width needed to ensure equilibrium. For the third failure mode, the output is also the location of the critical rupture line along the rear side wall, e.g. ABCD on Figure 2.

Earth pressure and bearing capacity

The total earth pressures discussed above are computed by integrating the unit earth pressures along the failure planes assumed, and where the associated earth pressure coefficients are derived in accordance with [3], Mortensen & Krogsbøll (2019). Note that [3] deviates from EN 1997-1, Appendix C.2 by introducing an earth pressure coefficient for the γ-case, K_γ using $K_\gamma = K_p$ for

the active case (K_p refer to surcharge case) while $K_\gamma = K_p/\cos\delta$ for the passive case, which is an approximation not deviating more than 4 % from the theoretically correct value provided that φ' ≤ 45° and the soil surface is horizontal.

The drained bearing capacity formula follows DS/EN 1997-1 DK NA:2021, [4] and only the unit weight and surcharge contributions have been shown for plane strain corresponding to normal eccentricities, e/BB ≤ 0.30:

$$\frac{V}{b_{eff}} = 0.5 \cdot \gamma' \cdot b_{eff} \cdot N_\gamma \cdot i_\gamma + q' \cdot N_q \cdot i_q \quad (2.1)$$

where b_{eff} = BB - 2·e (effective foundation width), γ' is the effective unit weight, $N_\gamma = 0.25 \cdot ([N_q - 1] \cdot \cos\varphi')^{3/2}$, $i_q = (1 - H/V)^2$, $i_\gamma = i_q^2$, q' is the effective surcharge load at foundation level, $N_q = \tan^2(45° + \varphi'/2) \cdot e^{\pi \cdot \tan\varphi'}$. When the normalised eccentricity, e/BB exceeds 0.30 (strong eccentricity), the bearing capacity failure mechanism is a rotational mechanism below the foundation and Equation (2.1) turns into $V/b_{eff} = \gamma' \cdot b_{eff} \cdot N_\gamma \cdot i_\gamma$.

3. RESULTS

Main tendencies from the results analysing a series of different geometries have been included below. Figure 3 shows the failure mechanisms developed around an L-shaped gravity walls with the height HH = 5.0m and foundation width varying between 5.0 and 1.0m. The L-shaped walls are placed directly on the soil surface, so the bearing capacity of the walls is a pure γ-case (no soil cover on the front side of the wall).

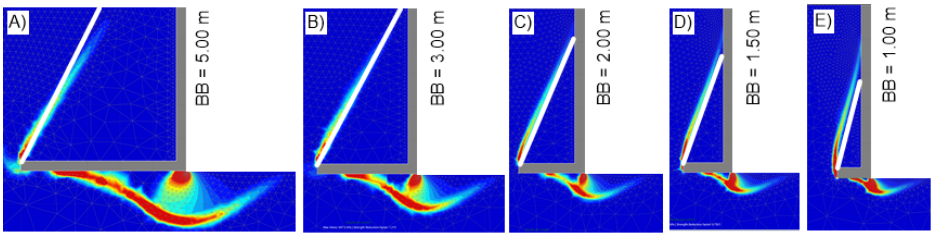

Figure 3. Contour plots of mobilised shear stress as found by Optum^{G2} in coarse grained soils. The white line from the rear side heel refer to the inclination of the critical rupture line found from the third failure mode in the Limit Equilibrium Method.

Failure of the structures in Optum^{G2} was introduced by gradually reducing the friction angle until a mechanism has developed, and the corresponding failure value of φ' was then used in the Limit Equilibrium Methods to estimate the required heel length B1 on Figure 2, Part 1. Figure 4 is established as Figure 3, but the wall is embedded into the soil and a toe has been introduced.

Main results from 12 different cases covering walls placed at the soil surface, embedded walls, and walls with and without surcharge loading are: The sum of foundation widths from the 12 cases in Optum^{G2} adds up to 33.2m. The corresponding value from the DK approach leads to 37.9m (+12% relative to

Optum^{G2}), the UK approach sums up to 37.5m (+14%) and the third Limit Equilibrium Method arrives at 37.0m (+11%). The three Limit Equilibrium Methods uses the same computational approach when estimating the bearing capacity and the passive earth pressure so any difference in results must reflect a difference in the way the active earth pressure is estimated, and no practical difference is observed. The estimated value of the total active earth pressure from the three different Limit Equilibrium Methods is not affected by the degree of sophistication applied in the various models. It is therefore suggested to use the UK model when evaluating the active earth pressures as this involves rather simple calculations.

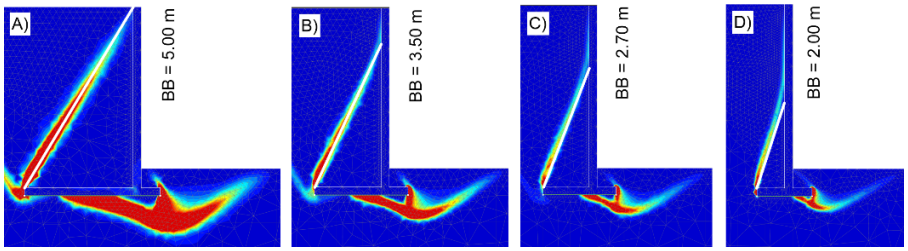

Figure 4 Contour plots of mobilized shear stress using Optum^{G2} in coarse grained soils. The white line from the rear side heel refer to the inclination of the critical rupture line found from the third failure mode in the Limit Equilibrium Method.

Figure 4, Case A) represents a rupture line from the rear side heel to the top of the wall and the inclination of this rupture line with horizontal is close to the statically admissible angle being $\pi/2-\varphi'/2$. There is a vague tendency in the results obtained that the DK method leads to shorter heels than the UK method when the angle between the heel and the line from the rear side heel to the top of the wall exceeds the statically admissible angle and opposite if it doesn't. This tendency is, however, not very strong and it will not change the recommendation about the UK method being the preferred method.

Figure 3 refer to cases where the wall is placed at the soil surface and the bearing capacity is therefore a pure γ-case. The active pressures from Figure 3, Case A) and B), when estimated by Optum^{G2}, must be almost identical to the values found using the UK method so any difference in results comparing the heel length from Optum^{G2} and the heel length from the UK method must be found in the bearing capacity formula, Equation (2.1). The bearing capacity factor from Optum^{G2} was therefore estimated for a centrally loaded foundation placed on a coarse grained soil with no surcharge using associated flow to check the validity of the program. Optum^{G2} found $N_\gamma = 14.8$ for $\varphi' = 30°$ while the value from Equation (2.1) is 14.6 showing a close match. The Finite element method and Equation (2.1) therefore seems to deviate on the inclination factor, i_γ. Steenfelt (2003), [5], suggested that $i_\gamma = (1 - 0.7 \cdot H/V)^5$ should be used in Equation (2.1) and Table 1 illustrates the effect of the different inclination factors.

Table 1 Main results for Figure 4 case A) using Optum^{2G} and the UK method with two different inclination factors.

	BB [m]	b_{eff} [m]	V/b_{eff} [kPa]	H [kN/m]
Optum^{G2}	5.00	4.39	131	117
UK, $i_\gamma = (1 - 0.7 \cdot H/V)^5$	5.38	4.72	117	106
UK, $i_\gamma = (1 - H/V)^4$	5.67	5.05	116	106

Optum^{2G} results in Table 1 are found by integrating effective normal stresses and shear stresses along the interface between the soil and the bottom part of the foundation. A similar approach has also been used on rupture figures depicted in Figure 3, Part E) and Figure 4, Part D) revealing that b_{eff} / BB > 0.30. This ratio reflects a strong eccentricity, cf. Equation (2.1), and the failure mode in the soil below the wall should reflect a clockwise rotation of the wall, which is not observed from the contour plots (but found in the Limit Equilibrium Methods).

4. WATER PRESSURES AROUND THE WALL

The presence of water around the structure will influence the design. Drains may be used to control the water pressure but as the lifetime of a drain is typically shorter than the lifetime of the structure, drains cannot be assumed to be fully operational. Differential water pressures will cause a steady state flow situation where water will typically flow from the rear side of the wall towards the front side. This effect will cause a destabilising horizontal force from water combined with hydraulic gradients influencing the effective unit weight and thereby also influencing the active and passive earth pressures. Piping/erosion may develop on the front side of the wall and as the base plate act a membrane, water pressures below the plate will act upwards, cf. Figure 5 (Left), and these pressures will influence the vertical reaction, V on Figure 2 together with the overturning moment.

5. DISCUSSIONS AND CONCLUSIONS

Discussions, Associated flow versus non-associated flow

The finite element analyses included in this paper has consistently been conducted assuming associated flow; that is to use the same angle of dilatancy as the friction angle, $\psi = \varphi'$ and it deviates from non-associated flow where $\psi < \varphi'$. Using finite element analysis to verify the earth pressure coefficients from EN 1997-1 Appendix C.2 reveals that associated flow must be used, which is also the case for the bearing capacity factors in Equation (2.1). From testing in

the geotechnical laboratory, it is known that real soils behave as non-associated materials, and it is also known that non-associated analyses will lead to a lower resistance than associated material when using the same friction angle. The designer must therefore account for these aspects when deriving characteristic values of the shear strength properties if simple design tools are to be used.

Figure 5 (Right) has been based on a series of 2D Plaxis analysis where the ULS resistance has been computed using associated and non-associated flow ($\psi = \varphi' - 30°$ [industry practice]). The figure allows for transforming friction angles from non-associated flow to associated flow for active earth pressures, passive earth pressures and for the bearing capacity.

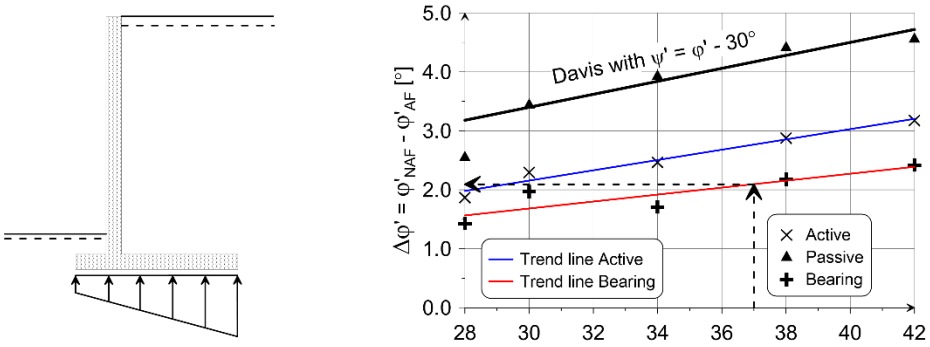

Figure 5 Left: Vertical water pressures acting on the base plate caused by differential water pressures acting on the wall. Right: Simplified method to evaluate the effect of associated flow versus non-associated flow.

The x-axis on Figure 5 (Right) represents the friction angle from non-associated flow, φ'_{NAF} while the y-axis represents $\Delta\varphi' = \varphi'_{NAF} - \varphi'_{AF}$ where φ'_{AF} is the friction angle for associated flow. It is seen that $\varphi'_{NAF} = 37°$ (and thus $\psi = 7°$) leads to the same bearing capacity as $\varphi'_{AF} = 37\text{-}2.1 = 34.9°$. The line "Davis" follows $\tan\varphi'_{AF} = \sin\varphi'_{NAF}\cdot\cos\psi/[1 - \sin\varphi'_{NAF}\cdot\sin\psi]$ using $\psi = \varphi'_{NAF} - 30°$ and has been suggested by [6], Davis (1968). The Plaxis analyses with passive pressures in Figure 5 (Right) are based on the pure γ-case without surcharge. The active pressures and the bearing capacities in the same figure have been computed using $\gamma' = 10$ kN/m^3, a foundation width (or wall height) of 3.0 m and a surcharge of 15 kPa.

Discussions, Robustness

A structure is robust when the safety is only slightly sensitive to unintended effects and defects or, when there is no extensive failure of the structure if a limited part of the structure fails, cf. [7], DS/EN 1990 DK NA.

A critical aspect for most gravity walls is a reduced soil resistance caused by flowing water on the front side of the wall and below the base plate. Such

events must be mitigated by establishing a sufficient soil cover in front of the wall and ensuring that the design water tables have been set conservatively. The roughness of the front side wall and/or along the foundation base should be re-considered if the wall fails in sliding. If the ALS or robustness analysis reveals a wall failing by bearing pressures combined with a strong eccentricity, extreme care should be exercised as all partial safety factors are unity (no safety) and because a possible failure will likely develop without a detectable warning, e.g. settlements / displacements.

Conclusions

For design of gravity walls, the UK approach (active failure boundary as vertical line from heel extreme) should be the preferred design approach as it is very easy to use, and it does not imply cumbersome evaluations of triangular stiff soil bodies and earth pressures along inclined lines; both aspects shall be re-computed for every heel length evaluated to establish the final design.

The cases studied implies that the largest difference between finite element analysis and the limit equilibrium methods originate from the bearing capacity equation applied. The Danish bearing capacity equation, as it appears in EN 1997-1 DK NA:2021, should thus be re-evaluated.

Characteristic values of the soil properties shall account for differences between associated flow and non-associated flow depending on the tool applied in the design. Using a design tool reflecting associated flow, the soil properties on the passive side should be carefully evaluated.

Water tables must be selected conservatively taking the lifetime of the structure into account. The effect of flowing water shall be considered carefully.

REFERENCES

[1] Optum^{G2}, Version 2019.02.19, Optum Computational Engineering, www.Optumce.com.

[2] Plaxis 2D, Version 8.6, www.plaxis.nl.

[3] Mortensen N. & Krogsbøll A. (2019). Effect of tangential surface load components on earth pressure coefficients, Proc., 17th ECSMGE, Iceland.

[4] DS/EN 1997-1 (National annex from 2021 included).

[5] Steenfelt J. S. (2003) Critical examples of shallow foundations design, Symposium International FONDSUP 2003, Paris.

[6] Davis E. H. (1968). Theories of plasticity and failure of soil masses. *Soil Mechanics, selected topics*, I.K. Lee, Butterworths, London. p341-381.

[7] DS/EN 1990 DK NA:2021.